UNESCO Chair on
Coastal Geo-Hazard Analysis
Research Institute for Earth Sciences
Geological Survey of Iran

unesco
Chair

Abstract:

Until now, due to the lack of complete and detail studies of the geotechnical behavior of the foundation and the existence of factors such as; determining the bearing capacity of soil, liquefaction and immediate and long-term settlement, many civil and economic resources have been destroyed. On the other hand, considering that Iran is an earthquake-prone region, investigating the behavior of the load-bearing capacity of layers under the foundation during an earthquake is of particular importance.

By identifying the various factors that reduce soil resistance, the best method can be chosen to improve soil properties and increase its resistance. But first of all, it is necessary to identify the areas prone to this phenomenon. This research can provide the possibility of zoning the region in terms of problematic soils.

ISBN: 978-622-5858-88-6

2024

unesco
Chair
UNESCO Chair on
Coastal Geo-Hazard Analysis
Research Institute for Earth Sciences
Geological Survey of Iran

UNESCO Chair on
Coastal Geo-Hazard Analysis
Research Institute for Earth Sciences
Geological Survey of Iran

unesco
Chair

Stratigraphy and Engineering Parameters of the Quaternary Deposits of South Caspian Sea Region (Gilan Province)

UCCGHA 022

2024

Stratigraphy and Engineering Parameters of the Quaternary Deposits of South Caspian Sea Region (Gilan Province)

سرشناسه : بهروی‌فر، ساره، ۱۳۶۷-
Behravifar, Sareh, 1988

عنوان و نام پدیدآور : Stratigraphy and engineering parameters of the quaternary deposits of South Caspian Sea region (Gilan Province)[Book]/ authors Sareh Behravifar; employer Research Institute for Earth Sciences, Geological survey of Iran; summarized and translated into English Manouchehr Ghorashi; supervisors Fereydon Rezaei, Mahmoudreza Majidi fard, Afshin Karimkhani; with cooperation UNESCO Chair on Coastal Geo-Hazard Analysis.

مشخصات نشر : تهران: نشر خزه، ١٤٠٣ = ٢٠٢٤ م.

مشخصات ظاهری : ۷۸ ص.؛ ۱۴/۵ × ۲۱/۵ س‌م.

شابک : 978-622-5858-88-6

وضعیت فهرست نویسی : فیپا

موضوع : چینه‌شناسی – پارامترهای مهندسی – رسوبات کواترنری – دریای خزر -- بندر انزلی

موضوع : Stratigraphy – Engineering parameter – Quaternary deposite – Caspian sea -- Bandare Anzali

یادداشت : کتابنامه، ص. ٦٤ - ۷۸

شناسه افزوده : قرشی، منوچهر، ۱۳۲۰-، مترجم

شناسه افزوده : Ghorashi, Manouchehr

شناسه افزوده : یونسکو. کرسی مخاطرات زمین شناختی ساحلی

شناسه افزوده : UNESCO Chair on Coastal Geo-Hazard Analysis

شناسه افزوده : سازمان زمین‌شناسی و اکتشافات معدنی کشور. پژوهشکده علوم زمین

شناسه افزوده : Geological Survey & Mineral Exploration of Iran. Institute of Earth Sciences

رده بندی کنگره : QE۶۵۱

رده بندی دیویی : ۷۰۹۵۵۲۳۴۷/۵۱

شماره کتابشناسی ملی : ۹۵۲۶۸۳۹

Stratigraphy and Engineering Parameters of the Quaternary Deposits of South Caspian Sea Region (Gilan Province)

Author:

Sareh Behravifar

نشر خزه

اطلاعات گزارش

عنوان: چینه‌نگاری و بررسی پارامترهای مهندسی نهشته‌های کواترنری جنوب باختری کاسپین (محدوده انزلی)

مجری: پژوهشکده علوم زمین، سازمان زمین‌شناسی و اکتشافات معدنی کشور

زبان مرجع: فارسی

خروجی: گزارش، نقشه، مقاله، داده های الکترونیکی

ناظران علمی: فریدون رضایی، محمودرضا مجیدی‌فرد، افشین کرم‌خانی

نویسندگان: ساره بهروی‌فر

رئیس کرسی یونسکو در مخاطرات زمین شناختی ساحلی: حمید نظری

مسئول شورای اجرایی: راضیه لک

خلاصه‌نویسی و ترجمه به انگلیسی: منوچهر قرشی

ناشر: نشر خزه

با همکاری کرسی یونسکو در مخاطرات زمین شناختی ساحلی

چاپ اول: ۱۴۰۳

شمارگان: ۵۰ نسخه

صفحات: ۷۸

شابک: ۶-۸۸-۵۸۵۸-۶۲۲-۹۷۸

khazepub@gmail.com

Report Information

Title: Stratigraphy and Engineering Parameters of the Quaternary Deposits of South Caspian Sea Region (Gilan Province)

Employer: Research Institute for Earth Sciences, Geological survey of Iran

Original language: Persian

Output: Report, Map, Paper, Digital Meta Data

Supervisors: Fereydon Rezaei, Mahmoudreza Majidi fard, Afshin Karimkhani

Authors: Sareh Behravifar

Chairholder in the UNESCO Chair on Coastal Geo-Hazard Analysis: Hamid Nazari

Head of the Executive Council: Razyeh Lak

Summarized and translated into English: Manouchehr Ghorashi

Publisher: Khazeh Publication

with cooperation UNESCO Chair on Coastal Geo-Hazard Analysis

First Edition: 2024

Edition number: 50

Page: 78

Shabak: 978-622-5858-88-6

khazepub@gmail.com

Scientific Council

Name	Affiliation
Ara Avagyan	IGS: Institute Geological Sciences
Rick J Bailey	IOC-UNESCO Indian Ocean Tsunami Warning and Mitigation System/ UNESCO
Aram Fathian Baneh	University of Calgary
Wenjiao Xiao	Chinese Academy of Sciences
Magdi Guirguis	Institut français d'archéologie orientale du Caire
Richard Walker	University of Oxford
Philippe Agard	University of Sorbonne
Justin Ahanhanzo	Intergovernmental Oceanographic Commission of UNESCO (IOC-UNESCO)
Alice Aurelie	UNESCO Water Sciences Division
Eric Barrier	University of Sorbonne
Jean-François Ritz	University of Montpellier
Martin Hanz	German under water archaeology association
Klaus Reicherter	Aachen University
Judith Thomalsky	German Archaeological Institute Tehran Branch
Hamid Alizadeh Lahijani	Iranian National Institute for Oceanography and Atmospheric Science
Abbas Banj Shafiei	Urmia University
Yahya Djamour	Shahid Beheshti University (SBU)
Hassan Fazeli Nashli	University of Tehran
Razyeh Lak	Research Institute for Earth Sciences
Mohammad Mokhtari	International Institute of Earthquake

	Engineering and Seismology
Hamid Nazari	Research Institute for Earth Sciences
Jafar Omrani	Geological Survey of Iran
Morteza Talebian	Research Institute for Earth Sciences
Mohammad Tatar	International Institute of Earthquake Engineering and Seismology
Mahdi Zare	International Institute of Earthquake Engineering and Seismology
Stefano Salvi	National Institute of Geophysics and Volcanology (INGV)
Ryo Anma	Tokushima University
Yeong Bae Seong	Korea University
John Lambert	Deltares, UNESCO
Issa El-Hussain	Sultan Qaboos University
Ekkehard Holzbecher	German University of Technology in Oman
Egor Krasinskiy	Underwater research center Russian Geographical Society
Audemard Franck A.	Department of Geology, Central University of Venezuela
Executive Committee	
Name	**Affiliation**
Nasir Ahmadi	Environmental Protection Organization of Mazandaran Province
Arash Amini	Golestan University
Alireza Amrikazemi	Scientific Coordinator, Qeshm Island UNESCO Global Geopark
Parviz Armani	Imam Khomeini International University
Ataollah Dadashpour	Geological Survey of Iran, Sari branch

Asghar Dolati	Kharazmi University
Hasan Fazelinashli	University of Tehran
Fahimeh Foroghi	Iranian National Institute for Oceanography and Atmospheric Science
Abdolazaim Ghanghormeh	Golestan University
Habibolah Ghasemi	Shahrood University of Technology
Mohammad reza Ghasemi	Research Institute for Earth Sciences
Manouchehr Ghorashi	Research Institute for Earth Sciences
Jafar Hassanpour	University of Tehran
Ataollah Kavian	Environmental Protection Organization of Mazandaran Province
Mohammadreza Kazemzadeh	Superme Audit Gourt
Razyeh Lak	Head of RIES and Executive Manager
Mahmoudreza Majidifard	Research Institute for Earth Sciences
Ali Akbar Momeni	Shahrood University of Technology
Babak Moradi	Iranian National Institute for Oceanography and Atmospheric Science
Seyed Mohsen Mortazavi	Hormozgan University
Hasan Nasrollah Zadeh Saravi	Caspian Sea Ecological Research Center
Ehsan Pegah	Kharazmi University
Abdolwahed Pehpouri	Qeshm Island UNESCO Global Geopark
Ahmadreza Rabani	University of Science and Technology of Mazandaran
Mahdi Rahmanian	Shargh Daily newspaper
Ahmad Rashidi	International Institute of Earthquake Engineering and Seismology
Masoud Sadri Nasab	University of Tehran
Mohammad Salamati	Respina Company

Mohammad Tatar	International Institute of Earthquake Engineering and Seismology
Alireza Vaezi	Research Institute for Earth Sciences
Mojtaba Yamani	University of Tehran
Ahmed Hadidi	German University of Technology in Oman (GUTECH)
Secretariat	
Name	**Affiliation**
Elnaz Aghaali	Research Institute for Earth Sciences
Keivan Ajdari	Research Institute for Earth Sciences
Hourieh AliBeygi	Research Institute for Earth Sciences
Sedigheh Ghanipour	Research Institute for Earth Sciences
Hamoon Memarian	Research Institute for Earth Sciences
Shirin Safavi	Research Institute for Earth Sciences
Aazam Takhtchin	Research Institute for Earth Sciences
Mehrnoosh Pour Saeid	Graphic Designer
Hanieh Bakhshaei	Geological Survey of Iran
Reza Behbahani	Geological Survey of Iran
Javad Darvishi khatooni	Geological Survey of Iran
Mohammadreza Ensani	Geological Survey of Iran
Marziyeh Estrabi Ashtiyani	Geological Survey of Iran
Gholamreza Hoseinyar	Geological Survey of Iran
Mojtaba Kavianpour Sangno	Geological Survey of Iran

Contents

1 Introduction 1

2 Research objectives: 2

3 Physical and mechanical properties of soil layer 3

3.1- Soil bearing capacity 3

3.2- Bearing capacity equations 8

3.3- Liquefaction phenomenon 12

4 Stratigraphy of the Quaternary deposits of South west of the Caspian Basin. 19

4.1- Introductions 19

4.2- Relative age of the AREA NO. ONE sediments. 20

4.3- Relative age of the area no. two sediments 24

4.4- Relative age of the area no. three deposits 28

4.5- Relative age determination of sediments of the studied area 30

5- Conclusion and Discussion 35

Determination of engineering parameters of the area understudy 38

Area No. 1: 38

Area No. 2: 45

Area No. 3: 48

Suggestions 63

References 64

Table of Figures

Figure 1: Data collection location in area number 1 (WWW.GoogleEarth.com) 21
Figure 2: Comparing the columns of area number one......... 23
Figure 3: Data collection location in area number 2 (WWW.GoogleEarth.com) 25
Figure 4: Comparison of the stratigraphic columns of area No. 2 27
Figure 5: Data collection location in area number 3 (WWW.GoogleEarth.com) 29
Figure 6: Comparison of the stratigraphic columns of area No. 3 30
Figure 7: The location of the studied points in the region 32
Figure 8: Comparison of the columns of all three areas of the region 33
Figure 9: Comparison of the stratigraphic columns of the studied area with Antonian Paluska's stratigraphic column. . 34
Figure 10: Integration of sedimentology and engineering data in core number 1 37
Figure 11: The three-dimensional view resulting from the interpolation of information for soil consistency using information interpolation, in the (WWW.Golden Software Surface 10.com), where the horizontal axis (X,Y) indicates the coordinates of the boreholes and the vertical axis (Z) indicates the soil consistency in the UTM coordinate system. . The vertical column indicates the soil consistency scale calculated by the method (Hansen, 1970) with a rectangular cross section. 44
Figure 12: The three-dimensional view resulting from the interpolation of information for soil consistency using information interpolation in (WWW.Golden Software Surface

10.com), where the horizontal axis (X,Y) indicates the coordinates of the boreholes and the vertical axis (Z) indicates the soil consistency in the UTM coordinate system.............. 47
Figure 13: The distribution of boreholes in area No. 3 (Bandar Anzali) in Google Earth software 49
Figure 14: Three-dimensional view of the data obtained from the integration of the bearing capacity using Rezaei (2010) bearing capacity software, In SP soils in the city of Bandar-e-Anzali in the software (WWW.Golden Software Surface 10.com) where the horizontal axis (x,y) indicates the coordinates of the boreholes and the vertical axis (z) indicates the bearing capacity in terms of (kg/cm2) and in the UTM coordinate system. The vertical column indicates the bearing capacity scale calculated by the Hansen (1970) method in a rectangular cross section. 53
Figure 15: Diagram No. 4-1: Liquefaction of borehole 1 based on the standard penetration number with a maximum acceleration of 0.3 g and a magnitude of 7 Richter earthquake (soil liquefaction evaluation software based on SPT, Rezaei, 2010). 56
Figure 16: Diagram No. 4-2- Liquefaction of borehole 11 based on the standard penetration test with a maximum acceleration of 0.3 g and a magnitude of 7 Richter earthquake (soil liquefaction evaluation software based on SPT, Rezaei, 2010). 57
Figure 17: Diagram 4-3: Liquefaction of borehole 16 based on the standard penetration number with a maximum acceleration of 0.3 g and a magnitude of 7 Richter earthquake (soil liquefaction evaluation software based on SPT, Rezaei, 2010). 58
Figure 18: Three-dimensional view of the studied area based on problematic soils in (WWW.Golden Software Surface 10.com), where the horizontal axis (X,Y) indicates the

coordinates of the boreholes and the vertical axis (Z) indicates the problematic soils in the UTM coordinate system. is....... 62

Table of Table

Table 1: The interpolation and determination of C and φ values 40

1 Introduction

Until now, due to the lack of complete and detail studies of the geotechnical behavior of the foundation and the existence of factors such as; determining the bearing capacity of soil, liquefaction and immediate and long-term settlement, many civil and economic resources have been destroyed. On the other hand, considering that Iran is an earthquake-prone region, investigating the behavior of the load-bearing capacity of layers under the foundation during an earthquake is of particular importance.

By identifying the various factors that reduce soil resistance, the best method can be chosen to improve soil properties and increase its resistance. But first of all, it is necessary to identify the areas prone to this phenomenon. This research can provide the possibility of zoning the region in terms of problematic soils.

By examining the soils of the study area in terms of stratigraphic compliance as well as soil mechanics tests, preliminary and sometimes comprehensive information will be provided to researchers. In this project, engineering and geological features have been investigated in parts of the Bandar-e-Anzali, quadrangle map, scale 1:250.000, namely around the Anzali laguna, between Fuman and Masal, and Anzali city. It is worth noting, that from the morphological Point of view, Bandar-e- Anzali quadrangle consists of three distinct zones:

1- Coastal Caspian

2- Chenier (coastal plain)

3- mountainous.

2 Research objectives:

- Litho-stratigraphy of the Quaternary sediments in the studied area.
- Correlation of various stratigraphic sections.
- to study the geotechnical characteristics of soils.
- Preparing hazard vulnerability zonation map (liquefaction, settlement…)

3 Physical and mechanical properties of soil layer

In order to determine the physical characteristics of the soil layers, the usual granulation tests and determination of the Atterberg limits (fluidity and plasticity limits of the soil) have been performed on the samples taken from different depths of the boreholes. Based on the results of the above tests and according to the unified classification, the fine-grained layers of the boreholes are in the rows of CL (clay with low plasticity properties), CH (clay with high plasticity properties) and MH (elastic silt) and granular layers in the row is SP (sand with poor grain size), SM (sandy silt), SP-SM (sand with poor grain size with silt) and GP (gravel with bad grain size sand).

3.1- Soil bearing capacity

The bearing capacity of the soil can be explained according to the type of foundation of the structure under construction.

An explanation of the foundations:

According to the definition of foundation, it is the underlying structure and part of the soil adjacent to it. Topic 7 of the National Building Regulations has also provided a similar result. A part of the foundation and the soil in contact with it, through which the load is transferred between the structure and the ground, is called a foundation. In fact, the task of the foundation is to transfer the loads of the upper parts to the soil under the foundation in such a way that excessive stresses and additional settlements are not created. Foundations can be divided into four categories:

1- Shallow (Surficial) foundations called surface foundations
2- Semi-deep foundations
3- Deep foundations
4- Special foundations: including any foundations that are not included in the above categories such as caisson foundations.

The type of foundation is selected based on structural information, soil engineering properties, economic considerations and implementation issues. The minimum steps required to design a surface foundation can be summarized as follows:

1- Determining the depth of the foundation: This depth is determined based on the prevention of soil erosion under the foundation, environmental factors, frost depth, etc. The depth of the foundation should be lower than the area that undergoes a large volume change due to the change in monsoon humidity. Also, the foundation should be away from the penetration of plant roots. The minimum foundation depth is usually considered to be 0.7 meters to one meter (Roshan Zamir, 2012).
2- Determining the dimensions of the foundation plan (floor dimensions): In this step, it is assumed that the foundation is capable of bearing the incoming loads.
3- Checking the overall settlement and unequal settlement: both of these settlements as well as the rotation and distortion of the footing

should be within the permissible values of the regulations.

4- Structural design or determining the thickness and amount of required rebar: it is assumed that the dimensions of the foundation are sufficient and the soil does not break, and structural element is able to withstand the incoming loads.

According to steps 2 and 3, the foundation soil must be able to withstand the loads caused by any engineering structure that is built on it without suffering shear failure. In addition, the resulting settlements must be bearable for the desired structure.

The shear failure of the foundation soil can cause the building to tilt or even overturn. Additional settlement can also damage the building frame, and problems such as locking of doors and windows.

It is rare to find a structure that has collapsed due to shear failure of the foundation. Most of the reported shear ruptures are related to the foundations of embankments or similar structures, in which the reliability coefficient is considered relatively low. So most of the construction problems and defects are caused by poor foundation design due to time-dependent settlements.

For any structure, it is necessary to check both shear strength and settlements. In many cases, the settlement criteria control the permissible bearing capacity, although at the same time, there are cases where the shear strain of the foundation determines the proposed bearing capacity. For example, the permissible bearing capacity of foundations located on saturated cohesive soil is based on unconfined compressive strength. Structures built on soft soils, such as liquid storage tanks and flatten foundations, can be more settlement, especially if the structure is loaded in such a way that the settlement takes place uniformly.

It should be noted that although here the main focus is on the bearing capacity of the foundation of framed structures and machinery foundations, the same methods can be used to determine the bearing capacity of foundations of other structures such as foundations of towers, dams and embankments. The bearing capacity of layered soils and foundations located in the vicinity of slopes is also investigated in this study.

The permissible design bearing (qa) capacity is selected based on the minimum value of the following two items.

1- The final bearing (qult) capacity based on the shear strength of the soil, which is divided by a suitable confidence factor, the permissible bearing capacity is determined as follows:

$$qa: qult/SF$$

2- The contact pressure resulting from limiting the settlement to a permissible value.

3.2- Bearing capacity equations

Currently, there is no any method to determine the bearing capacity except as an estimate. Vesik (1973) tabulated 15 theoretical solutions Since 1940 and excluded at least one of the more common methods. Since then, several other methods have been proposed. Among the many theories presented to determine the bearing capacity of the foundation, some have been widely used and have gained more popularity and validity. These methods include Terzaghi, Mirhoff, Hansen and Vesic analysis, which are discussed in this section.

Since the beneath of foundation is usually hard and dense (and if it is loose or soft, it is condensed or stabilized in some way), So in determining the bearing capacity, it is mainly assumed that the rupture is of the general shear type.

The difference between the various theories is mainly related to the difference in the shape and the direction of selected fracture surfaces.

Also, to simplify the problem to a two-dimensional state, the bearing capacity analysis mainly starts with the banded foundation, and then the necessary correction coefficients are applied to the shape of the foundation.

Tarzaghi bearing capacity equations

One of the most basic bearing capacity equations for banded foundations was proposed by Terzaghi

(1943). Tarzaghi's analysis is based on the following assumptions.

(A) The floor of the foundation is rough.

(B) The depth of the foundation is less than or equal to its width.

(C) The shear strength of the soil above the foundation floor level is ignored and this soil is replaced with a uniform pressure (overhead).

(D) The length of the foundation is long

(E) The load on the foundation is vertical and the contact pressure has a uniform distribution.

(F) The shear strength of soil is subject to the Mohr-Coulomb criterion.

Terzaghi's bearing capacity equation is as follows:

$$q_{ult} = cN_cS_c + \bar{q}N_q + 0/5_\gamma BN_\gamma S_\gamma$$

Meyerhoff bearing capacity equations

Meyerhoff (1951, 1963) proposed a bearing capacity equation similar to Terzaghi's equation, but he added a factor of the form Sq to the deep term, qN_q. He also considered deep coefficients di and inclination coefficients Ii for the case where the load deviates from the vertical.

Mayerhoff loading capacity are as follows:

vertical loading capacity

$$q_{ult} = cN_c s_c d_c + \bar{q} N_q s_q d_q + 0/5_{\gamma} \acute{B} N_{\gamma} s_{\gamma} d_{\gamma}$$

oblique loading capacity

$$q_{ult} = cN_c d_c i_c + \bar{q} N_q d_q i_q + 0/5_{\gamma} \acute{B} N_{\gamma} d_{\gamma} i_{\gamma}$$

The difference between the values obtained from the Meyerhoff and Terzaghi equations becomes apparent at great depths.

Hansen Bearing Capacity equation

Hansen's bearing capacity equations method is based on Meyerhoff (1951) method.

Hansen loading capacity equation:

$$q_{ult} = cN_c s_c d_c i_c g_c b_c + \bar{q} N_q s_q d_q i_q g_q b_q + \frac{1}{2} \gamma \acute{B} N_{\gamma} s_{\gamma} d_{\gamma} i_{\gamma} g_{\gamma} b_{\gamma}$$

Vesic Bearing Capacity equation

Vesic (1973, 1975) method is the same as Hansen's relations with some changes in the calculation of coefficients. The value of Nc and Nq are the same as Hansen's relations. But N_y proposed by Visk is slightly different.

$$N_\gamma = (1 + N_q) \tan \emptyset$$

3.3- Liquefaction phenomenon

If a loose sand mass is subjected to vibration, it tends to decrease in volume and density. If the sand is saturated under these conditions, the tendency to reduce the volume in the sand mass with a constant volume will increase the pore water pressure between the soil grains. Fine-grained sandy soils, due to their low permeability, do not have the ability to reduce the pressure in the pore water created at the same time as the vibrations occur, and this water pressure in the sand mass constantly increases. After a short period of time, a situation occurs where the pore water pressure becomes equal to the overburden pressure and the total stress on the soil element. As a result, the effective stress is equal to zero.

$$\acute{\sigma} = \sigma - u$$

In the above relation, σ' is effective stress, σ is total stress and u is pore water pressure. Granular soils, such as sand, are lack of cohesion, and as a result, their shear strength will only be caused by the friction between the grains. Therefore, the following relationship holds true for sandy soils:

$$\tau = \acute{\sigma} \cdot \tan \emptyset$$

In this regard, the τ is shear strength of sand, σ', the effective stress on the shear plan and Ø the angle of internal friction between the soil grains based on the effective stress.

According to the above two relationships, it can be seen that in the case that the pore water pressure is equal to or close to the overburden pressure, the effective stress will be equal to or close to zero, and consequently, the shear strength (τ) will also be close to zero in these sandy soils.

In such conditions, the saturated sands act as liquid and become liquid, that is why this phenomenon is called liquefaction.

After the liquefaction, the sand particles are deposited in the water and after the sedimentation is completed, the sand is in a denser state.

Seed (1985) listed the mechanisms related to liquefaction of saturated sand caused by earthquake as follows;

1- The vibrational motion of the earthquake causes periodic shear stresses in the saturated sand.

2- Shear stresses cause the tendency to shrink, but in undrained sand conditions, the volume change does not occur in the sand.

3- Subsequently, additional pore pressure is created in the sand and accumulates.

4- The effective stresses decrease and as a result the shear strength decreases.

5- Finally, if the additional pore pressure is high enough, the shear resistance will reach to a very low level and the soil will flow.

Resistance to shear strain or deformation also decreases as a result of increasing pore water pressure. The shear model (G) that controls the shear stresses is also a function of the average normal effective stress ($\sigma 1$) and therefore the shear modulus decreases with the increase in pore water pressure caused by an earthquake.

In dangerous cases, such as the Niigata earthquake, the sand acts like a liquid and caused disastrous results for the structures.

One of the main causes of damage during an earthquake is the rupture of the ground, which may be due to the loss of its resistance. This will be from saturated sandy lands due to pore water pressure and liquefaction phenomenon.

Several geological factors are involved in the rate of soil liquefaction potential, including the sedimentation process, age of sediments, geological history, depth of water table, grain size, depth of burial, slope and finally proximity to a free surface.

If liquefaction occurs in a soil and its shear resistance is lost, it may cause rupture in the lower layers. If structures have been built on such sedimentary layers or near them, there is a possibility of destroying of structures during the ground ruptures. ground ruptures have been divided into three categories based on the liquefaction phenomenon.

1- lateral expansion

2- flow fracture

3- loss of bearing capacity.

Lateral expansion is the movement of surface layers of soil parallel to the ground surface when there is a decrease in shear resistance in the lower layer due to the liquefaction phenomenon. Lateral expansion usually occurs on very gentle slopes with a slope of less than 5%. If differential lateral expansion takes place under a structure, the tensile stresses may be so great that the building breaks. It has been observed that flexible buildings tolerate such changes in tensile locations better than rigid buildings. Lateral expansion can have destructive effects on buried long and linear facilities (life-lines).

During the great 1906 San Francisco earthquake, it was observed that all water supply pipeline problems were caused by lateral failures. This made firefighting difficult during the earthquake and caused much of San Francisco to be destroyed by fire. Flow failures when large parts of the soil become liquefied or blocks of non-liquefied soil flow over a layer of liquefied soil. Landslides occur when the slope is greater than 5%. This phenomenon had disastrous effects during the 1964 Alaska earthquake. Liquefaction can also lead to a severe loos of the bearing capacity, which is usually accompanied by large deformations in the soil.

Structures buried in the soil may even be moved on the surface of the ground. In extreme cases, when the thickness of liquefied soils is high, tilting or overturning can occur. Such failures were observed during the 1964 Niigata earthquake in Japan. When the thickness of the liquefied soil is low or if a relatively thick non- liquefied soil is located on a liquefied sedimentary layer, strong tilting or overturning of structures will not occur, but there will be a possibility of vertical settlements.

Buried structures, such as underground tanks, may be subjected to more buoyancy because of the increase in pore water pressure due to the liquefaction phenomenon. Retaining structures, such as retaining walls or harbor structures, may be subjected to additional pressures caused by liquefaction in adjacent soils. The formation of soil settlement holes (when the sand boil phenomenon occurs), may cause settlement or tilting of structures located on surface foundations. Of course, the extent to which structures are directly or indirectly affected by failures caused by liquefaction depends on the extent of liquefaction. If liquefaction occurs in a thick horizontal sand layer, the associated effects on structures may be extensive. On the other hand, if the liquefaction is limited to very thin and discontinuous (lens) layers of the soil, the damage to the structures is minimal or even negligible.

In general, there are two ways to deal with the liquefaction phenomenon:

1- Soil strengthening i.e., improving soil conditions to minimize liquefaction phenomenon, 2- Structural strengthening by reducing the bearing capacity of the soil in the calculation and design of the foundation by using a deep foundation to transfer the forces to the lower layers of the soil where there is not liquefaction potential.

4 Stratigraphy of the Quaternary deposits of South west of the Caspian Basin.

4.1- Introductions

This chapter deals with Litho-stratigraphy https://www.antarcticglaciers.org/glacial-geology/techniques/lithostratigraphy/of the studied area. First, for each core of section we prepared a stratigraphy column. Each core section consists of various layers, with different characteristics. In area 1, samples collected around the Laguna consist mainly of sand, mud, plants and shell fragments.

In area 2, samples collected from rivers, which consist mainly of conglomerates, sand and mud. In area 3, Samples collected inside the Bandar-e Anzali. The aim of this chapter is, to study and correlate the columns of different areas, and to understand the litho-stratigraphy and relative age of the layers.

4.2- Relative age of the AREA NO. ONE sediments.

In this area, 21 cores, collected from environs and inside the Bandar-e-Anzali lagoon (Figure 1).

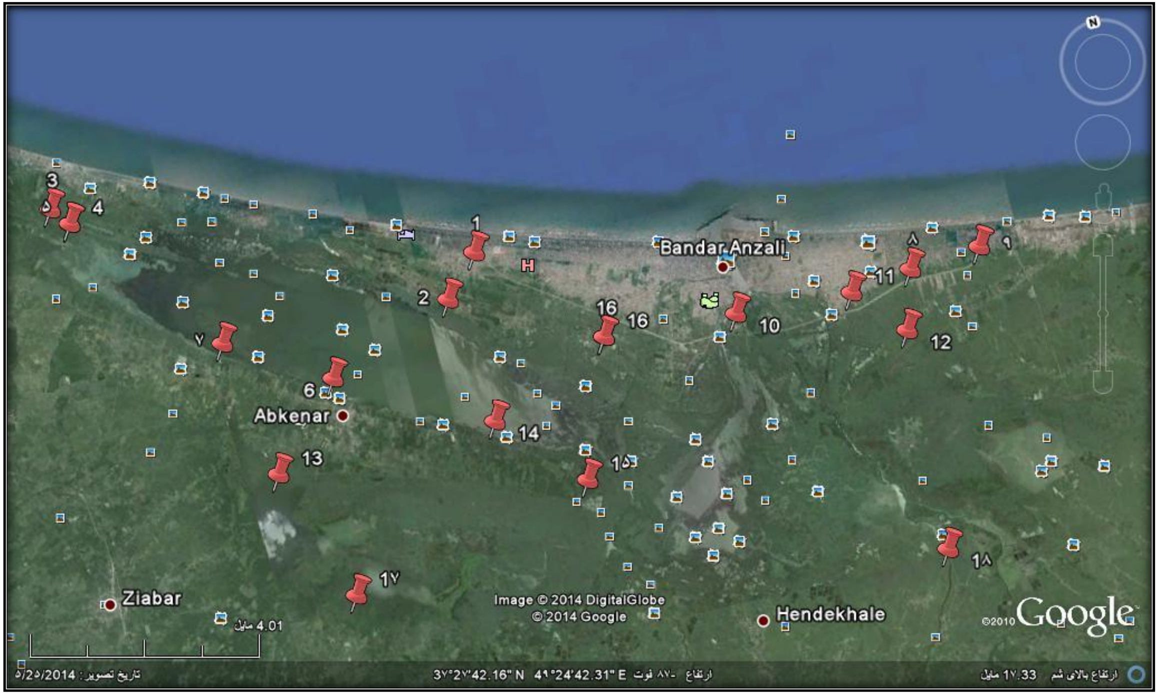

Figure 1: Data collection location in area number 1 (WWW.GoogleEarth.com)

Sediments of this area, consist mainly of sand, mud, plant and shell fragments, and gravel. Sediments from young to old (top to down) are as follows:

1- Man made soil or agricultural soil

2- Muddy deposits, with sand and sell and Plant fragments

3- Muddy - sand deposits

4- Muddy deposits with plant fragments

Comparative stratigraphy columns of area No. one shown in Figure 2.

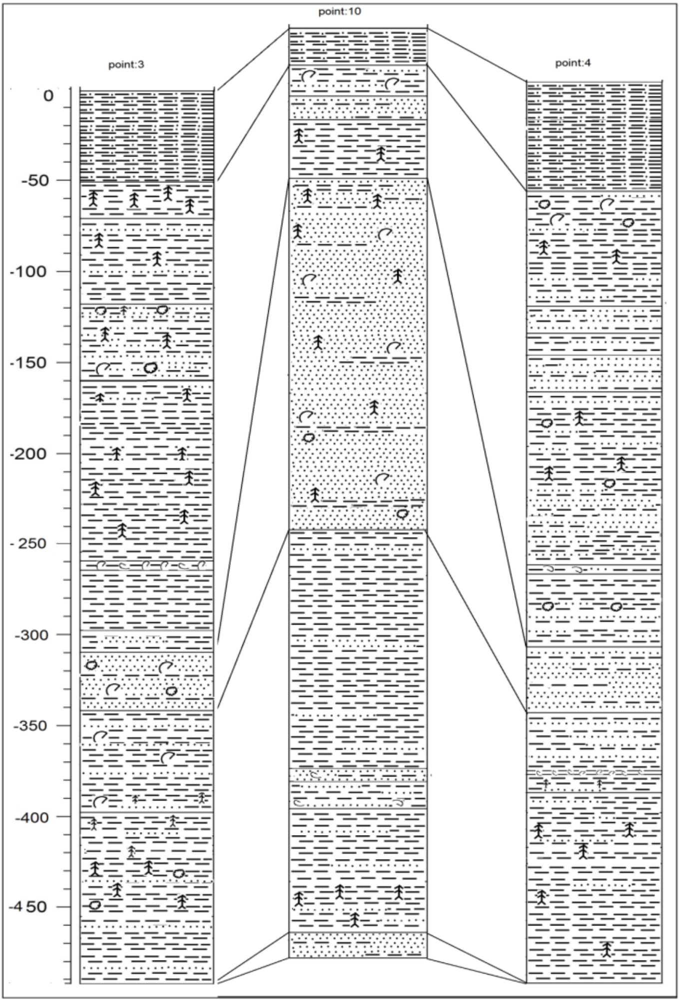

Figure 2: Comparing the columns of area number one

4.3- Relative age of the area no. two sediments

Deposits of this area (Figure 3) are mainly conglomerate, Sand and mud. Based on the Percentage of clasts, 3 types of conglomerates determined;

- type 1 (65+100) Percentage of clasts
- type 2 (30-65) Percentage of clasts
- type 3 (0-30) Percentage of clasts

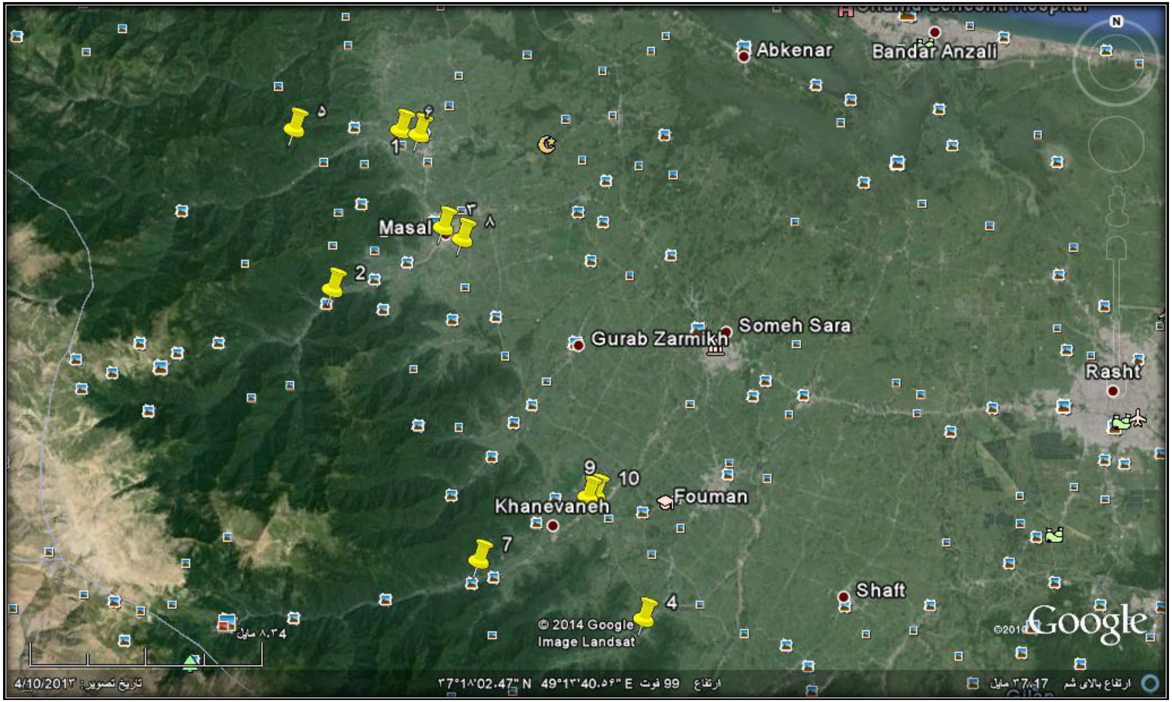

Figure 3: Data collection location in area number 2 (WWW.GoogleEarth.com)

The deposits of area no. 2, from Young to old (top to down) are as follows:

1- Man-made soil
2- Conglomerate
3- Mud sediment
4- Conglomerate
5- Mud or sand, with interbedded of conglomerate
6- Conglomerate

Comparative stratigraphy columns of area No. two shown in (Figure 4).

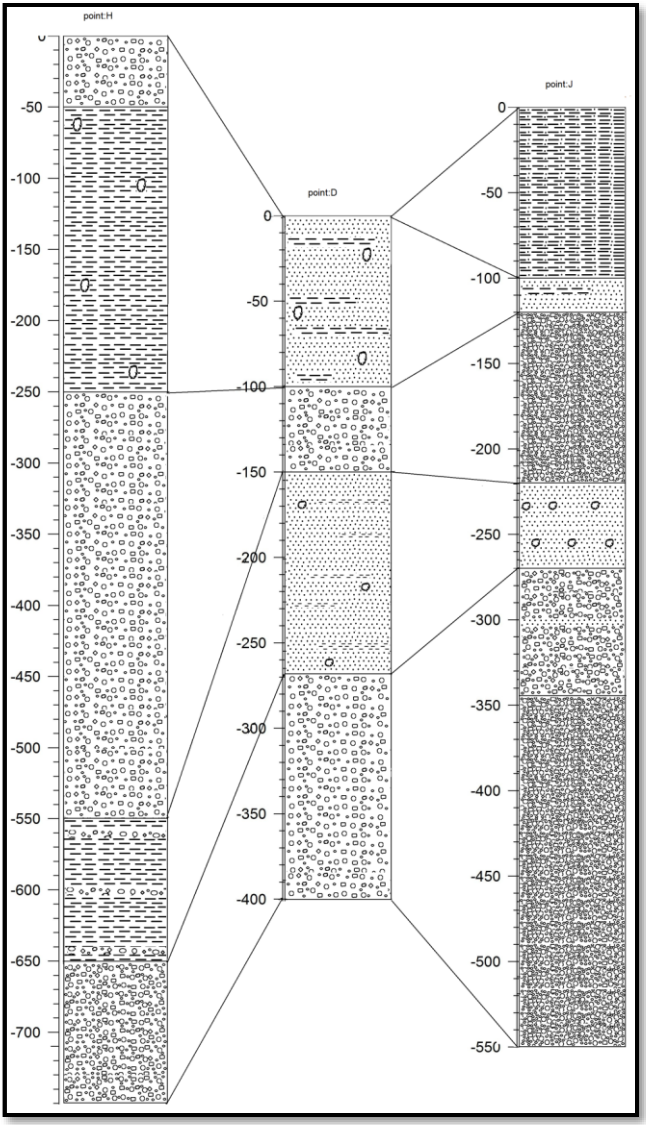

Figure 4: Comparison of the stratigraphic columns of area No. 2

4.4- Relative age of the area no. three deposits

Deposits of this area (Figure 5), From top to down (young to old) are as follows:

1- Man-made soil

2-Gravel and muddy sand

3-muddy sand with shell fragment

4- mud

5 muddy sand deposits

Comparative stratigraphy columns of area No. Three shown in Figure 6.

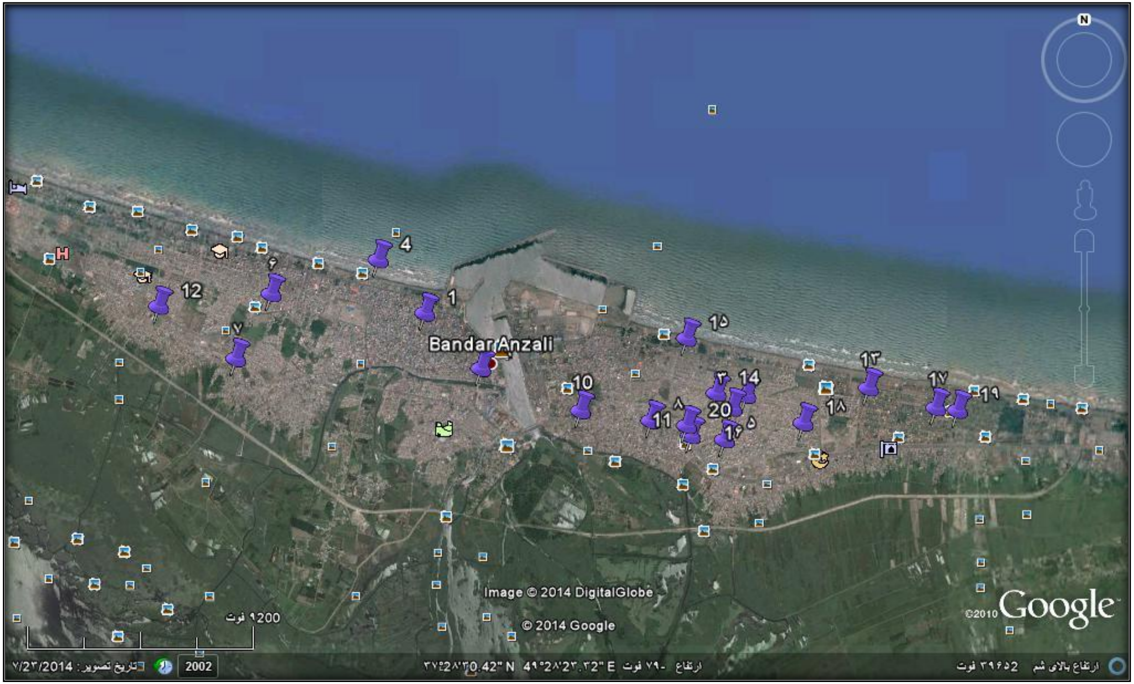

Figure 5: Data collection location in area number 3 (WWW.GoogleEarth.com)

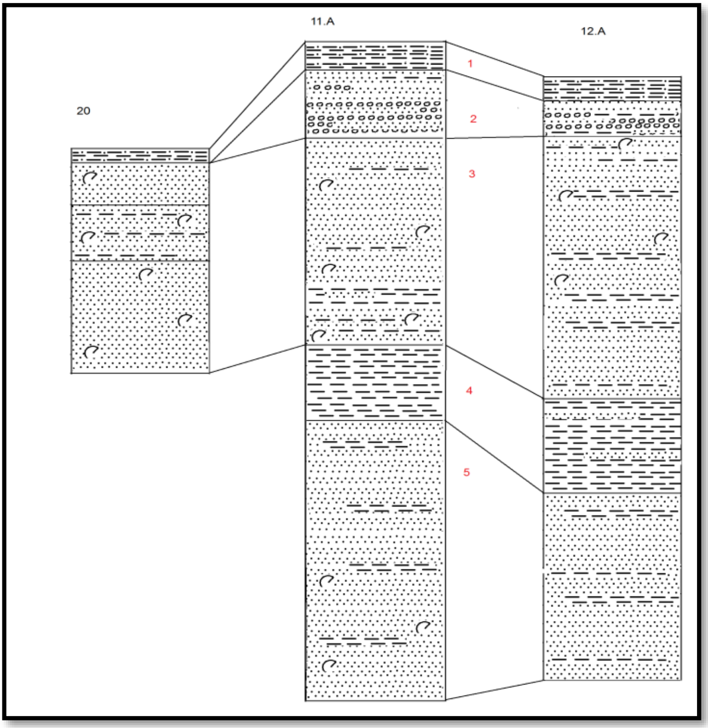

Figure 6: Comparison of the stratigraphic columns of area No. 3

4.5- Relative age determination of sediments of the studied area

The relative age of the sediments in whole area (Figure 7). From top to down (young to old) are as follows:

1- Man-made soil

2- Muddy sediments, with shell and plant fragment

3- Muddy sand with shell and plant fragments

4- Sandy mud

5- Muddy Sand

Figure 8 is comparative Columns of the whole area and Figure 9 is comparative columns of the studied area with stratigraphy column suggested by Paluska (1992).

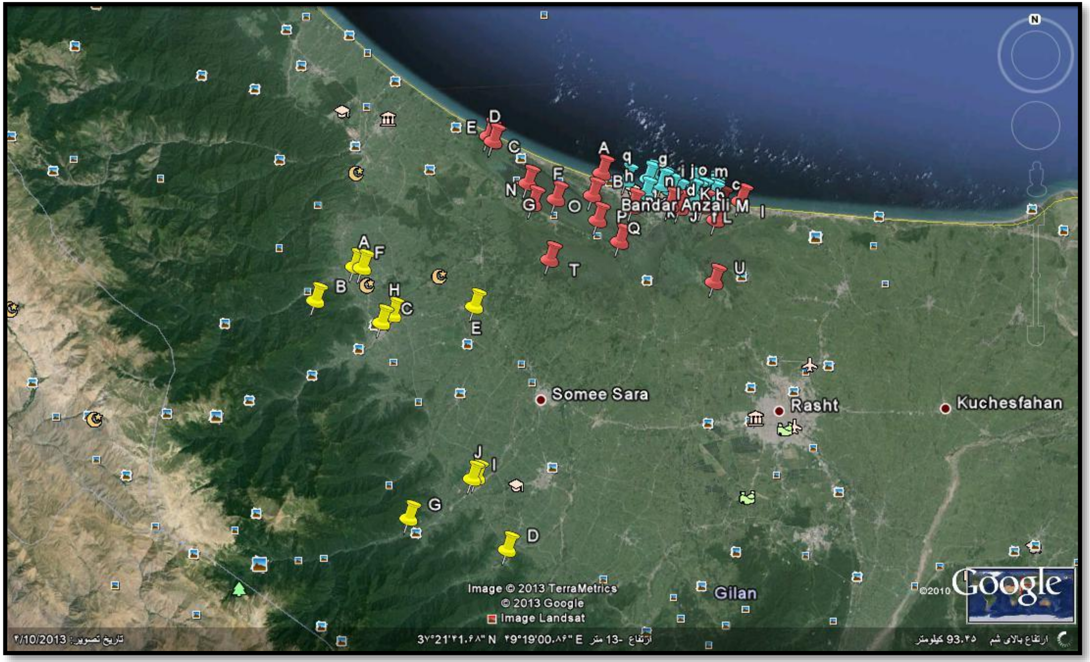

Figure 7: The location of the studied points in the region

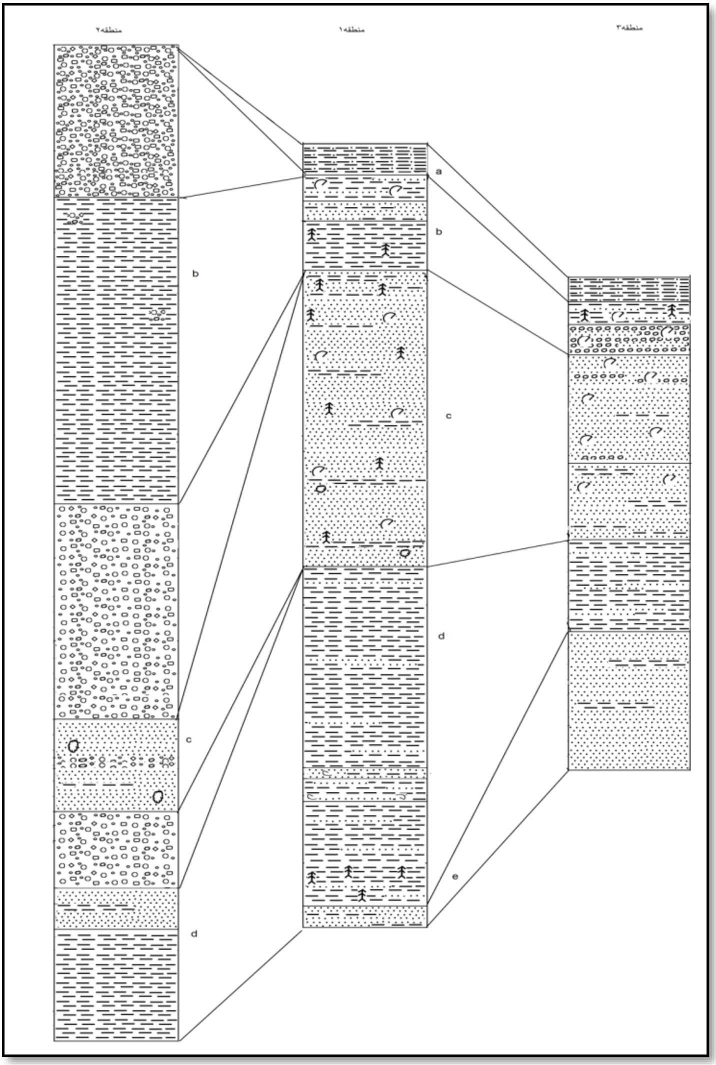

Figure 8: Comparison of the columns of all three areas of the region

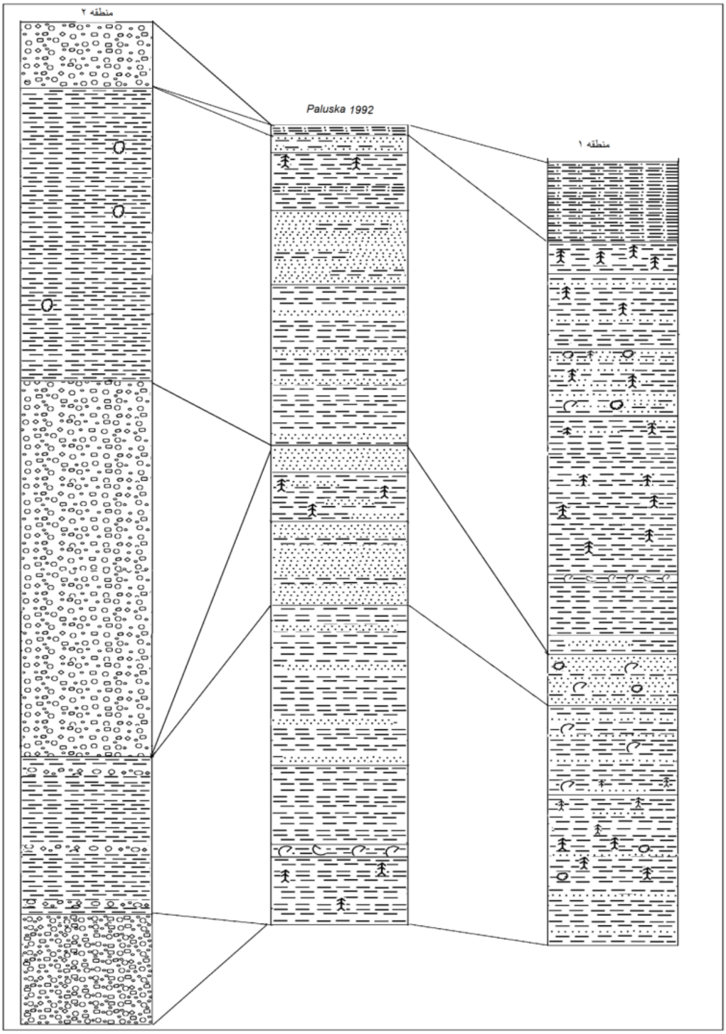

Figure 9: Comparison of the stratigraphic columns of the studied area with Antonian Paluska's stratigraphic column.

5- Conclusion and Discussion

The main results of this research are as follows:

- Drawing stratigraphical column for whole three areas of understudy

-Soil litho-stratigraphy determination of the area understudy.

Area No. one consists of 21 cores collected around Bandar-e-Anzali. The sediments consist mainly of sand, mud and gravel and are mostly diluvial- fluvial deposits.

Area No. Two consist of 10 cores mainly from river outcrops. Sections of this area consist of conglomerate, sand and mud. Based on the Percentage of clasts, three type of conglomerate recognized.

from Area No.3, consists of 20 cores, from inside, Bandar-e Anzali, and consist mainly of sand, mud and Gravel.

Relative age determination

In area NO. 1, deposits from top to down (young to old) are,

1. Man-made or agriculture soil,

2. Mud with shell and Plant fragments,

3- Sand,

4, Mud with shell and plant fragments

In area NO. 2, deposits from top to down (young to old) are,

1-Man-made Soil,

2-Conglomerate,

3-Mud with gravel,

4-Conglomerate,

5-Mud and sand with interlayer of conglomerate

In area NO.3, deposits from Top to down (young to old) are, (Figure 10)

1- Man-made Soil,

2- Gravel and sand with few mud,

3- Muddy sand,

4- Mud

5- Sand

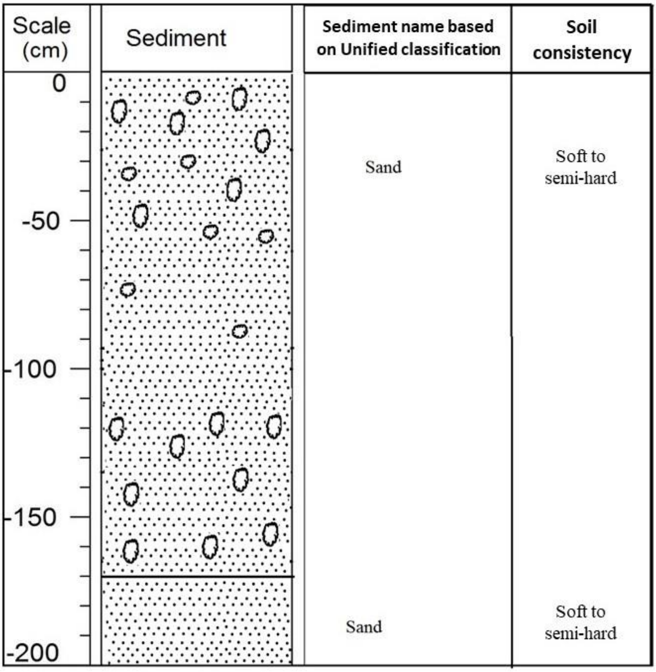

Figure 10: Integration of sedimentology and engineering data in core number 1

To compare deposits of all three areas, sediments from top to down (young to old) are as follows:

1- Man-made soil

2. Mud with shells and plant fragments with a few sand

3- Muddy sand, with shell and plant fragments

4- Sandy mud

5- Muddy sand

Determination of engineering parameters of the area understudy

Area No. 1:

According to the results of the soil grading samples by 3 charts (1- chart for determining the sign and name of the group for sandy and gravelly soils, 2- chart for determining the sign and group for clay and inorganic soils, 3- chart for determining the sign and name of the group for clay soils and organic layer), sediments were first named. Then, based on the obtained names and the weight percentage of clay, silt, sand and gravel, the values of the angle of internal friction (φ) and the value of adhesion (C) can be approximately determined and according to obtained values, the density and consistency of the soil can be interpolated. Fine grain particles are sticky and have low permeability. Coarse grain particles such as sand and gravel will have more resistance if they are cohesive, but if there is space between the particles due to the increase of water in the soil, there is a possibility of liquefaction. According to the type of soil and the percentage of coarse and fine particles, the amount of internal friction and adhesion is determined, and in conjunction to those two values, the density of the soil is determined, the higher the density, the higher the consistency of the soil. The interpolation and determination of C and φ values is done by the Table 1.

Table 1: The interpolation and determination of C and φ values

<table>
<tr><td colspan="5">Relative density of granular soil</td><td colspan="3">Soil type</td></tr>
<tr><td>I_D =</td><td>1</td><td>0.67</td><td>0.33</td><td>0</td><td></td><td></td><td></td></tr>
<tr><td>ϕ</td><td></td><td>40-45</td><td>37-40</td><td>35-37</td><td>gravel</td><td rowspan="4">non-organic</td><td rowspan="7">non-Cohesive soils</td></tr>
<tr><td>ϕ</td><td></td><td>38-40</td><td>35-38</td><td>32-35</td><td>sand: course & medium</td></tr>
<tr><td>ϕ</td><td></td><td>35-37</td><td>32-35</td><td>28-32</td><td>sand: fine & silty</td></tr>
<tr><td>ϕ</td><td></td><td>25-30</td><td>22-65</td><td>18-22</td><td>sand: organic</td></tr>
<tr><td colspan="5">Consistency of cohesive soil</td><td rowspan="3"></td><td rowspan="3"></td></tr>
<tr><td></td><td>stiff to very stiff</td><td>stiff</td><td>semi stiff</td><td>soft to very soft</td></tr>
<tr><td>n = W_s</td><td>I_e = 1</td><td>0.75</td><td>0.5</td><td>0</td></tr>
<tr><td>ϕ</td><td>24-28</td><td>22-24</td><td>19-22</td><td>5-19</td><td>sand with semi clay</td><td rowspan="3">non-organic</td><td rowspan="3">Cohesive soils</td></tr>
<tr><td>C'</td><td>30-40</td><td>20-30</td><td>15-20</td><td>2-15</td><td>silty sand</td></tr>
<tr><td>Φ_w</td><td>20-25</td><td>16-20</td><td>10-16</td><td>7-10</td><td>silts
I_p<10%</td></tr>
</table>

ϕ	22-26	19-22	15-19	12-15	sandy silt		
C'	40-50	30-40	20-30	3-20	silts sand- clayey		
					clayey silts		
Φ_w	16-20	12-16	7-12	5-7	silts I_p =10-20%		
ϕ	20-23	17-20	12-17	8-12	Sand, clay, silt		
C'	60-50	50-60	30-40	5-30	Silt & clay		
Φ_w	12-15	9-12	5-9	2-5	I_p = 20-30%		
ϕ	17-19	14-17	5-12	5-10	sandy clay, clay		
C'	60-80	50-60	40-50	10-40	clayey silt		
Φ_w	8-10	5-8	2-5	0-2	I_p > 30%		
Parameters of this group should be determined in Lab.					organic silt, peat, etc.	organic	

Soil consistency of area number 1

As already mentioned, while the soil mechanics tests have not been done for this area, it has been done to determine the liquefaction and looseness of the soil through information interpolation. For this purpose, the amount of soil consistency has been determined in the following intervals and the surfer software has been used to display the soil consistency in the area. Here is a 3D rendering of the survey results for the area (Figure 11).

Soft	$0 \leq \text{consistency} \leq 1$
Soft to semi-hard	$1 \leq \text{consistency} \leq 2$
Semi-hard to hard	$2 \leq \text{consistency} \leq 3$
Hard	$\text{consistency} \leq 4$

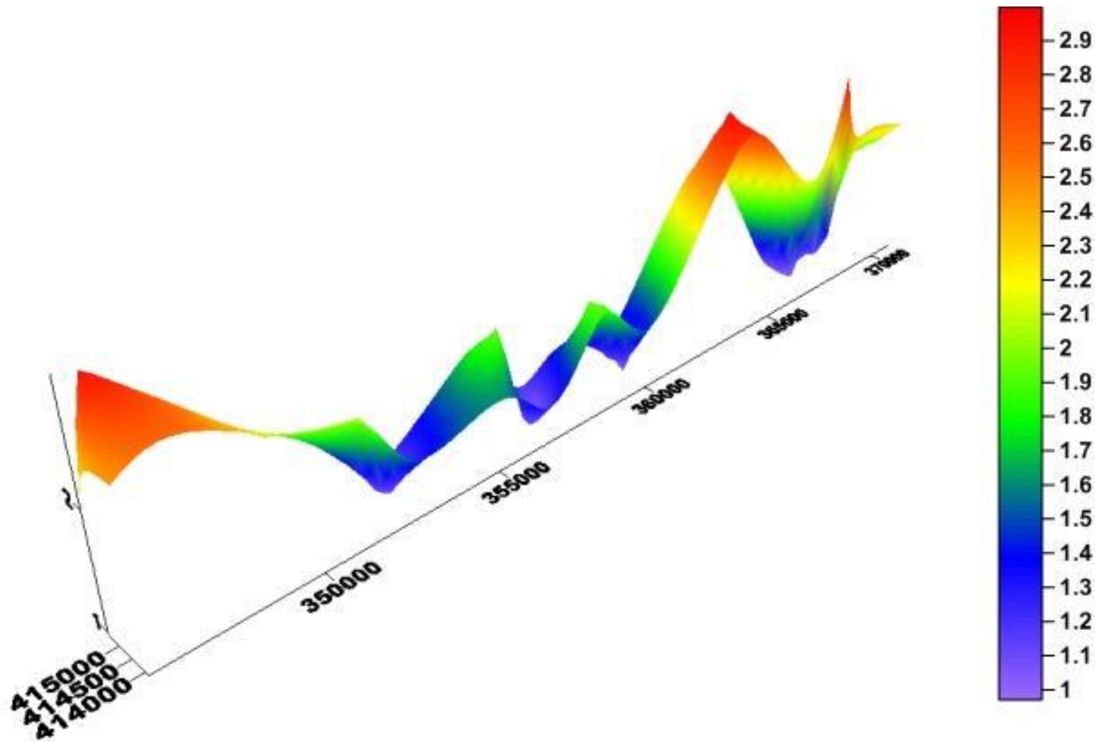
2.9
2.8
2.7
2.6
2.5
2.4
2.3
2.2
2.1
2
1.9
1.8
1.7
1.6
1.5
1.4
1.3
1.2
1.1
1
350000
355000
360000
415000
414500
414000

Figure 11: The three-dimensional view resulting from the interpolation of information for soil consistency using information interpolation, in the (WWW.Golden Software Surface 10.com), where the horizontal axis (X,Y) indicates the coordinates of the boreholes and the vertical axis (Z) indicates the soil consistency in the UTM coordinate system. . The vertical column indicates the soil consistency scale calculated by the method (Hansen, 1970) with a rectangular cross section.

Area No. 2:

In this area, since the sediments are related to the banks of the rivers, the amount of gravel is high. As in Section No. 1, the name of the soil is first determined by the soil naming tables, and then the required engineering information is interpolated by Table 1 and finally charts have been prepared for each section.

Soil consistency of area number 2

Soil mechanics tests have not been done in this area, so as a result, soil liquefaction and looseness have been determined through data interpolation (soil consistency) Figure 12.

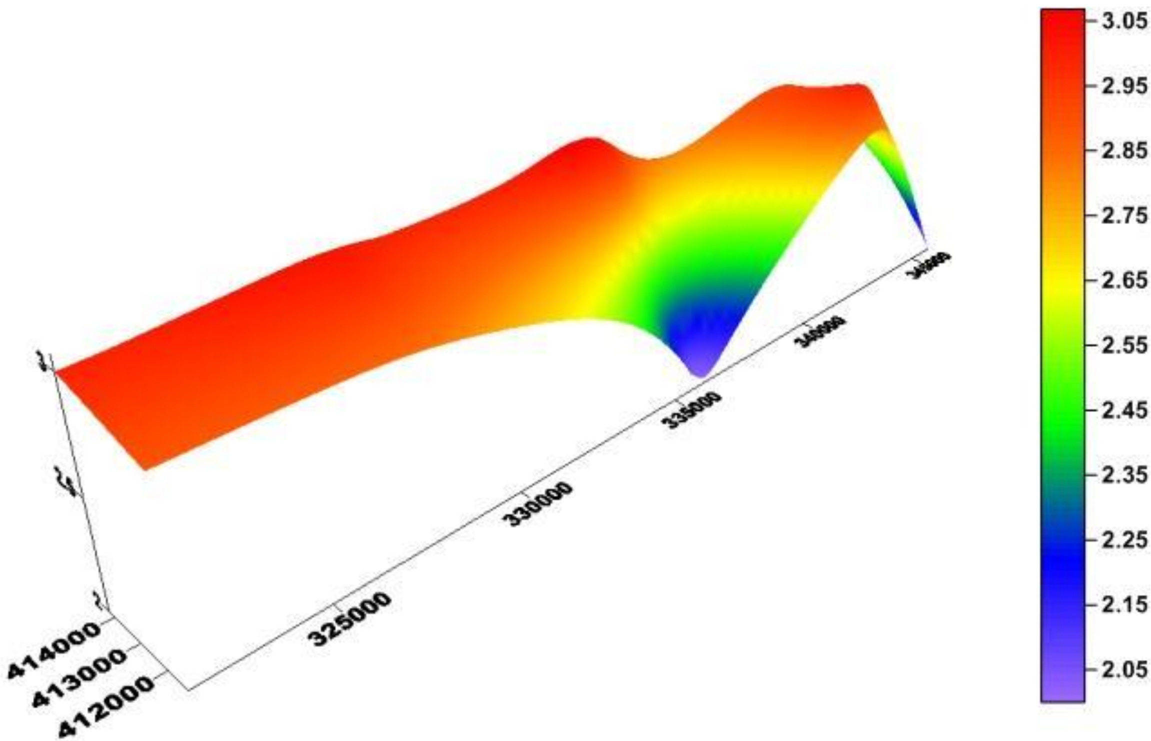
3.05
2.95
2.85
2.75
2.65
2.55
2.45
2.35
2.25
2.15
2.05
325000
330000
335000
414000
413000
412000

Figure 12: The three-dimensional view resulting from the interpolation of information for soil consistency using information interpolation in (WWW.Golden Software Surface 10.com), where the horizontal axis (X,Y) indicates the coordinates of the boreholes and the vertical axis (Z) indicates the soil consistency in the UTM coordinate system.

Area No. 3:

The information of this area includes the assessments made by Bandar-e-Anzali municipality to carry out construction projects. Soil mechanics tests have been performed on the collected samples. As a result, unlike the previous two areas where we had to interpolate information due to the lack of sufficient data, the required data is available in this area (Figure 13).

The following tests have been performed on all these projects:

- Index or physical tests: including the test to determine granulation, determine the limits of Atterberg, determine the specific weight of solid grains, permeability test and determine the percentage of natural moisture.
- Experiments to determine shear strength parameters: including direct shear test and triaxial test.
- A standard penetration test where the change in the number of SPT blows per 30 cm of penetration is determined.

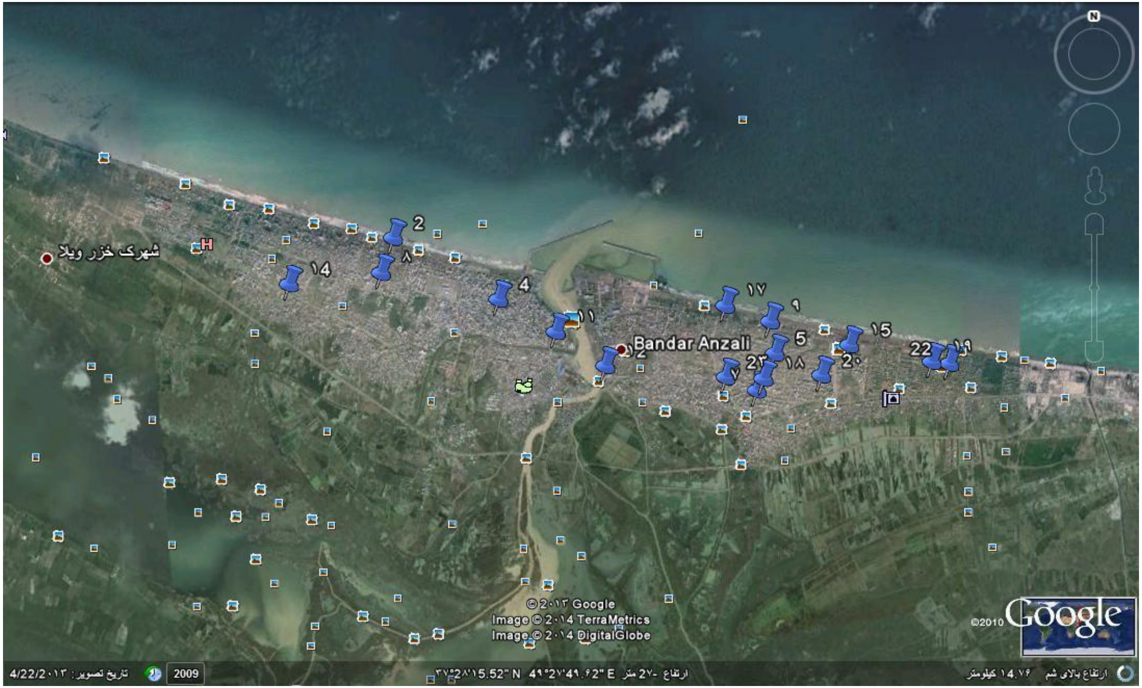

Figure 13: The distribution of boreholes in area No. 3 (Bandar Anzali) in Google Earth software

With the help of existing software's, the parameters of bearing capacity and liquefaction have been determined

Bearing capacity area No. 3:

The Permitted bearing capacity of foundations is evaluated by using the parameters of shear strength for surface foundations and by applying the confidence factor on the safe bearing capacity of the foundations, suggested by many researchers (e.g. Terzaghi bearing capacity, Meyerhoff bearing capacity, Hansen bearing capacity and Vesic bearing capacity).

In this project, the software prepared by Rezaei was used to calculate the bearing capacity, it should be noted that, this software was designed based on Hansen's method (Hansen, 1970).

Finally, according to the value of qa, the soil can be determined in terms of its problematic nature.

Weak and loose soil	$q_a \leq 1$
Medium to poor soil	$1 \leq q_a \leq 2$
Medium to strong soil	$2 \leq q_a \leq 3$
strong soil	$3 \leq q_a \leq 4$
Very strong soil	$q_a \leq 4$

Based on the calculations, the lowest -bearing capacity is 0.7 kg/cm^2 related to borehole 2 at a depth of 1.5 meters and the highest bearing capacity is 5 kg/cm^2 related to borehole 12 at a depth of 22 meters. The density, depth and loading level are different factors of bearing capacity results (Figure 14).

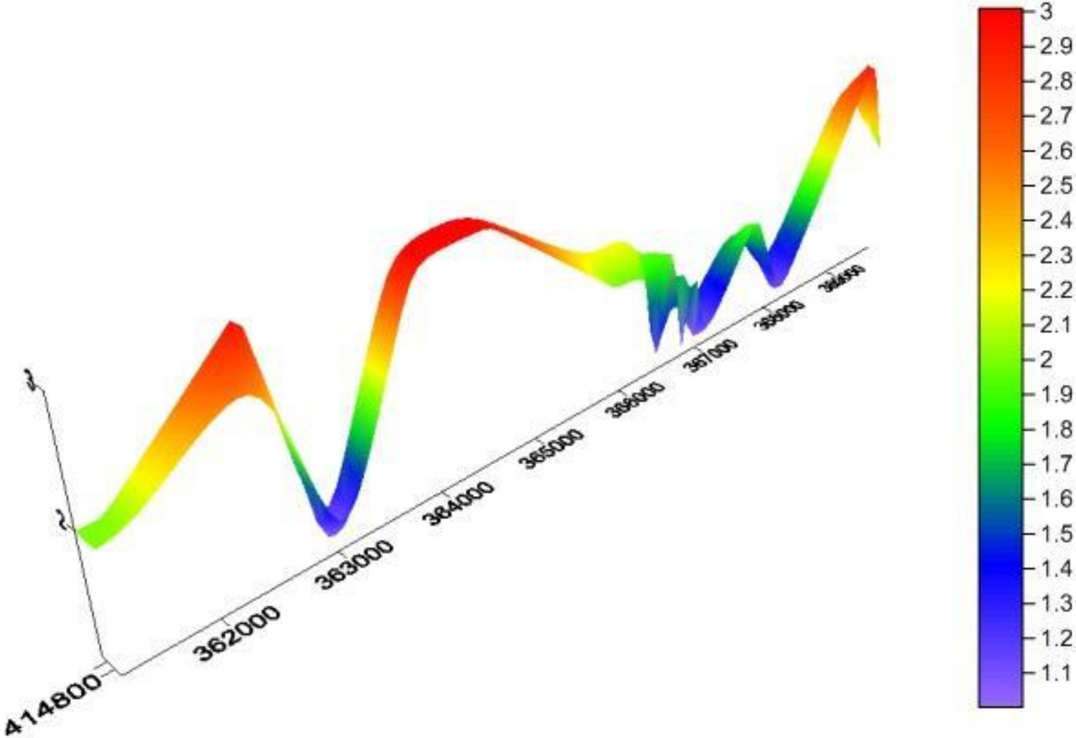
414800
362000
363000
364000
365000
367000
3
2.9
2.8
2.7
2.6
2.5
2.4
2.3
2.2
2.1
2
1.9
1.8
1.7
1.6
1.5
1.4
1.3
1.2
1.1

Figure 14: Three-dimensional view of the data obtained from the integration of the bearing capacity using Rezaei (2010) bearing capacity software, In SP soils in the city of Bandar-e-Anzali in the software (WWW.Golden Software Surface 10.com) where the horizontal axis (x,y) indicates the coordinates of the boreholes and the vertical axis (z) indicates the bearing capacity in terms of (kg/cm2) and in the UTM coordinate system. The vertical column indicates the bearing capacity scale calculated by the Hansen (1970) method in a rectangular cross section.

Liquefaction area No. 3:

To investigate the liquefaction phenomenon, another software developed by Rezaei (2019).

In this software, for each core with the sample prepared in the project, the data of the groundwater level in sample, the thickness of the sample layers, the amount of soil density (Y) in each layer, the value of SPT (N_{60}) in each layer and the percentage of grains passed through the 200 sieve in each layer are required. At the end, this software draws a diagram using the data used, which can be used to check the probability of liquefaction.

To calculate liquefaction for boreholes 1 to 25, grading curve, soil density based on soil type, standard penetration test, correction factor based on relative soil density and maximum ground acceleration (a_{max} :030) are considered.

(Software for evaluation of soil liquefaction based on SPT, Rezaei 2019) Liquefaction usually occurs in soils without uniform adhesion, whose 10% size is between 0.01 and 0.25 mm and its uniformity coefficient is between 2 and 10.

Due to the large number of samples, only a few of the results are shown here.

The underground water level is very important in the liquefaction factor, and considering that the underground water level in this borehole is at a depth of 2 meters, there is a possibility of liquefaction, but because the density of the soil is high, there is no possibility of liquefaction except at a depth of 10 meters (Figure 15).

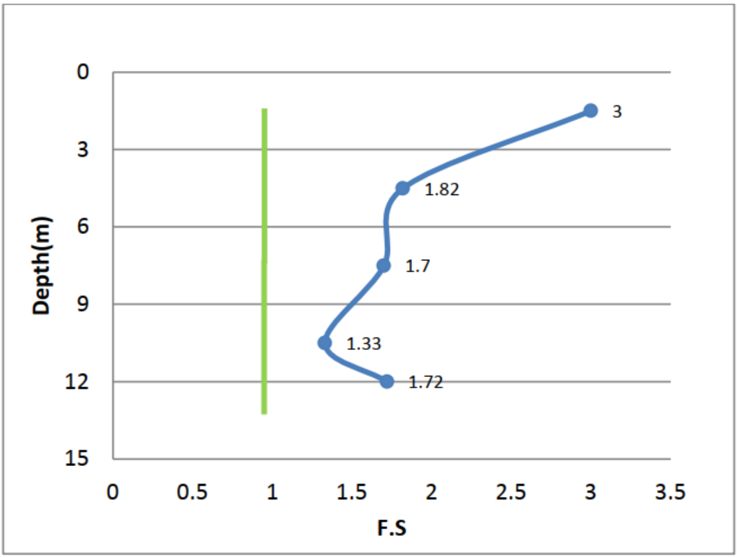

Figure 15: Diagram No. 4-1: Liquefaction of borehole 1 based on the standard penetration number with a maximum acceleration of 0.3 g and a magnitude of 7 Richter earthquake (soil liquefaction evaluation software based on SPT, Rezaei, 2010).

As can be seen in the diagram, liquefaction has occurred at a depth of 10 meters, but due to the type of soil, which is mostly coarse sand with high density, liquefaction potential will not be possible during an earthquake.

Considering that the underground water level in this borehole is at a depth of 1.8 meters and the soil is sandy, the possibility of liquefaction is high, but the presence of small sticky particles can reduce its intensity to some extent (Figure 16).

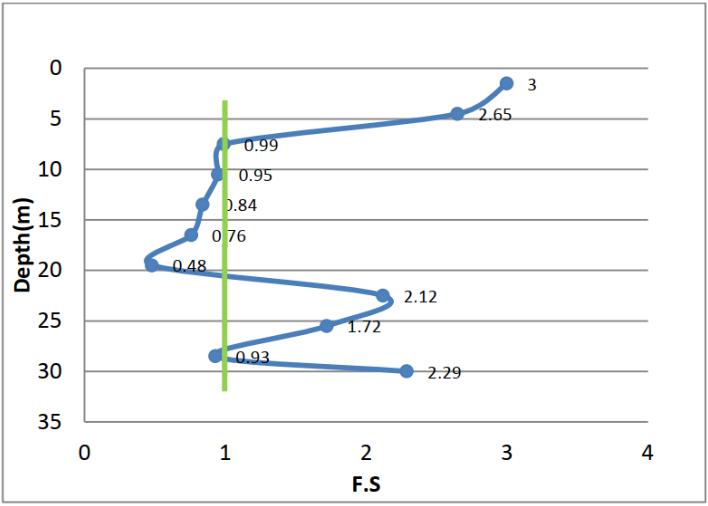

Figure 16: Diagram No. 4-2- Liquefaction of borehole 11 based on the standard penetration test with a maximum acceleration of 0.3 g and a magnitude of 7 Richter earthquake (soil liquefaction evaluation software based on SPT, Rezaei, 2010).

As can be seen in the diagram, the potential of liquefaction in some parts from a depth of 7 meters to a depth of 22 meters is possible, but due to the type of soil, which is mostly silty sand, the phenomenon of liquefaction during an earthquake will not be likely.

The underground water level in this borehole is at a depth of 2.5 meters, and due to the fact that the sand soil is poorly graded, the possibility of liquefaction is high (Figure 17).

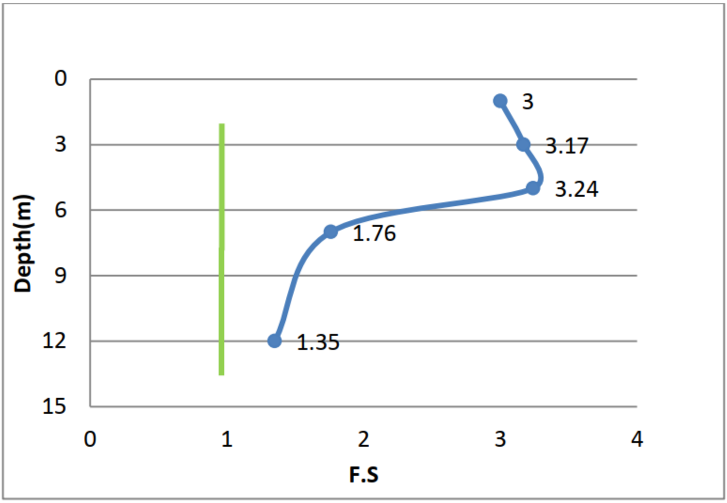

Figure 17: Diagram 4-3: Liquefaction of borehole 16 based on the standard penetration number with a maximum acceleration of 0.3 g and a magnitude of 7 Richter earthquake (soil liquefaction evaluation software based on SPT, Rezaei, 2010).

As can be seen in the diagram, there is a possibility of liquefaction at a depth of 10 meters, but on the basis of type of soil, which is mostly coarse sand but with high density, the phenomenon of liquefaction will not be likely during an earthquake.

Map of problematic soils in the region

This map is based on the surveys conducted in the studied region to provide a general and comprehensive view of the area and help to carry out construction activities as best as possible. As mentioned earlier, in this study, an attempt has been made to study the area both in terms of stratigraphy and engineering parameters. Soils that have low bearing capacity and fluidity, as well as soils with low consistency are considered as problematic soils, according to the reducing factors of these problems, the soil can be far away from being problematic or completely free of problems. Determining the problematic factors is the result of stratigraphy studies and engineering parameters in the region (Figure 18).

The result of the research and investigations of this project is the preparation of this map. The presented map covers the area of the studied area completely and has categorized and displayed the soils of the area in the following three groups:

1- Problematic soils

2- Slightly problematic soils

3- Soils without problems

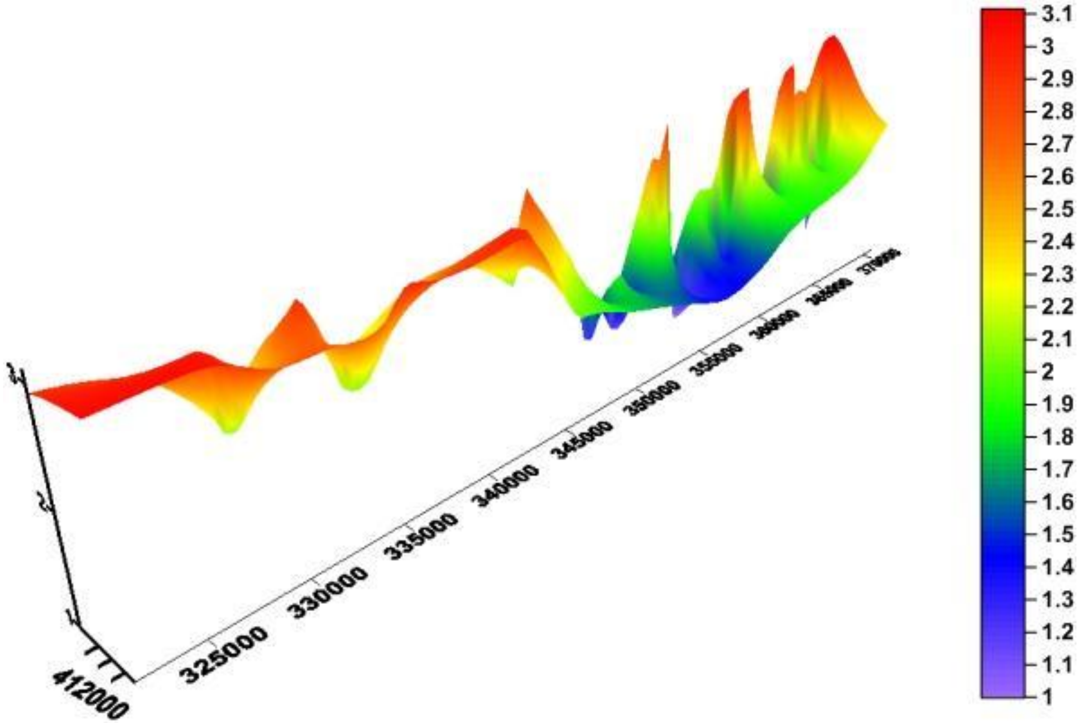
3.1
3
2.9
2.8
2.7
2.6
2.5
2.4
2.3
2.2
2.1
2
1.9
1.8
1.7
1.6
1.5
1.4
1.3
1.2
1.1
1
325000
330000
335000
340000
345000
350000
355000
360000
365000
370000
412000

Figure 18: Three-dimensional view of the studied area based on problematic soils in (WWW.Golden Software Surface 10.com), where the horizontal axis (X,Y) indicates the coordinates of the boreholes and the vertical axis (Z) indicates the problematic soils in the UTM coordinate system. is.

Suggestions

1- Radiometric dating will help for a better Understanding of stratigraphy sequences of the area,

2- We recommend soil mechanics tests for areas, number 1 and 2, in order to obtain more information

References

Bolton Seed, H., Tokimatsu, K., Harder, L.F. and Chung, R.M., 1985. Influence of SPT procedures in soil liquefaction resistance evaluations. Journal of geotechnical engineering, 111(12), pp.1425-1445.

Hansen, J.B., 1970. A revised and extended formula for bearing capacity.

Meyerhoff, R.W. and Smith, J.F., 1963. The thallium-indium phase diagram as a function of composition, temperature and pressure. Acta Metallurgica, 11(6), pp.529-536.

Paluska, Antoine, (translation by Shahrabi, M., 1992). Quaternary geology of the shores of the Caspian Sea, Geological Survey of Iran.

Rezaei, F., 2010, preparation of software for calculating soil liquefaction potential using SPT and CPT data. Research Institute for Earth Sciences.

Roshan Zamir, A., and Shokrani, Kh.M., 2003, Foundation Engineering, Danesh Harushan Berin, Negara

Terzaghi, K., 1943. Theoretical soil mechanics.

Vesic, A.S., 1975. Bearing capacity of shallow foundations. Foundation engineering handbook.